



Search for GeV Gamma-Ray Counterparts of Gravitational Wave Events with CALET/CAL

# CALET/CALによる重力波 イベントのガンマ線対応 天体探索

森 正樹

立命館大学工学部物理科学科

Masaki Mori for the CALET collaboration

マルチメッセンジャー天文学研究会2018, 千葉大学ハドロン宇宙国際研究センター、March 26-27, 2018

Multimessenger astronomy 2018, Chiba University

# CALET Collaboration



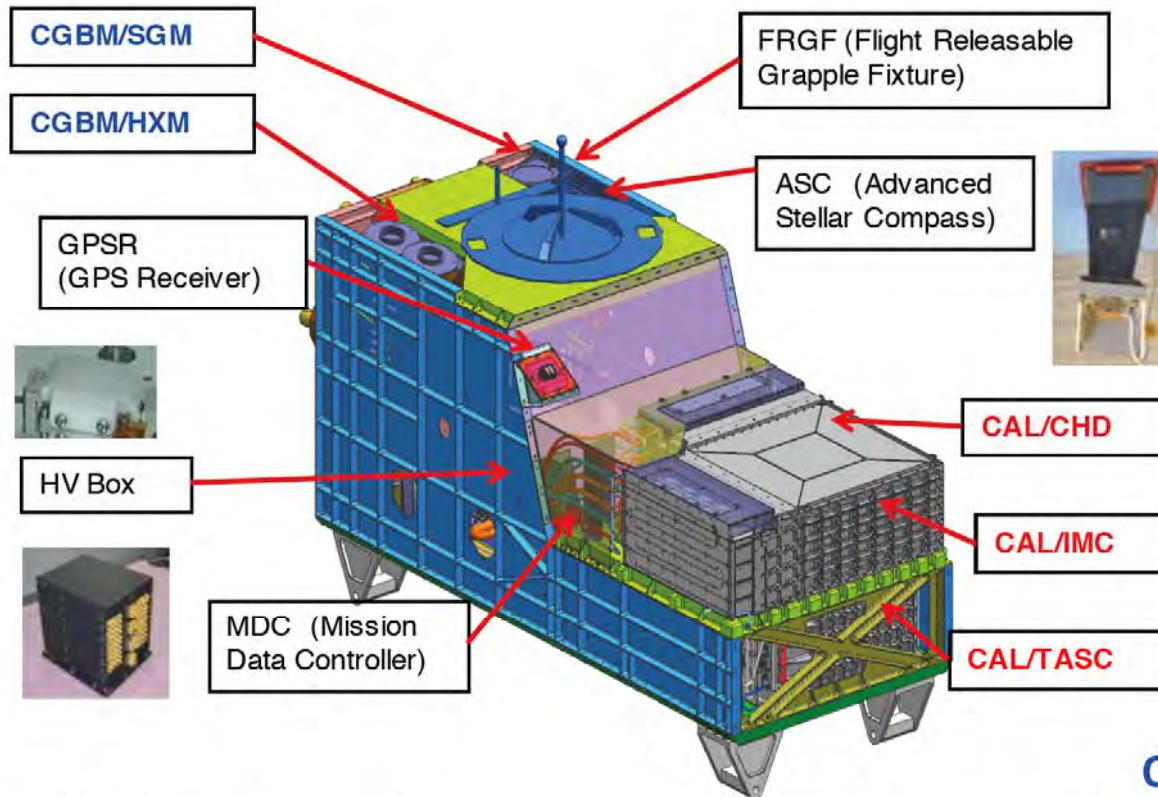
O. Adriani<sup>25</sup>, Y. Akaike<sup>2</sup>, K. Asano<sup>7</sup>, Y. Asaoka<sup>9,31</sup>, M.G. Bagliesi<sup>29</sup>, G. Bigongiari<sup>29</sup>, W.R. Binns<sup>32</sup>, S. Bonechi<sup>29</sup>, M. Bongi<sup>25</sup>, P. Brogi<sup>29</sup>, J.H. Buckley<sup>32</sup>, N. Cannady<sup>12</sup>, G. Castellini<sup>25</sup>, C. Checchia<sup>26</sup>, M.L. Cherry<sup>12</sup>, G. Collazuol<sup>26</sup>, V. Di Felice<sup>28</sup>, K. Ebisawa<sup>8</sup>, H. Fuke<sup>8</sup>, G.A. de Nolfo<sup>14</sup>, T.G. Guzik<sup>12</sup>, T. Hams<sup>3</sup>, M. Hareyama<sup>23</sup>, N. Hasebe<sup>31</sup>, K. Hibino<sup>10</sup>, M. Ichimura<sup>4</sup>, K. Ioka<sup>34</sup>, W. Ishizaki<sup>7</sup>, M.H. Israel<sup>32</sup>, A. Javaid<sup>12</sup>, K. Kasahara<sup>31</sup>, J. Kataoka<sup>31</sup>, R. Kataoka<sup>16</sup>, Y. Katayose<sup>33</sup>, C. Kato<sup>22</sup>, Y. Kawakubo<sup>1</sup>, N. Kawanaka<sup>30</sup>, H. Kitamura<sup>15</sup>, H.S. Krawczynski<sup>32</sup>, J.F. Krizmanic<sup>2</sup>, S. Kuramata<sup>4</sup>, T. Lomtadze<sup>27</sup>, P. Maestro<sup>29</sup>, P.S. Marrocchesi<sup>29</sup>, A.M. Messineo<sup>27</sup>, J.W. Mitchell<sup>14</sup>, S. Miyake<sup>5</sup>, K. Mizutani<sup>20</sup>, A.A. Moiseev<sup>3</sup>, K. Mori<sup>9,31</sup>, M. Mori<sup>19</sup>, N. Mori<sup>25</sup>, H.M. Motz<sup>31</sup>, K. Munakata<sup>22</sup>, H. Murakami<sup>31</sup>, Y.E. Nakagawa<sup>8</sup>, S. Nakahira<sup>9</sup>, J. Nishimura<sup>8</sup>, S. Okuno<sup>10</sup>, J.F. Ormes<sup>24</sup>, S. Ozawa<sup>31</sup>, L. Pacini<sup>25</sup>, F. Palma<sup>28</sup>, P. Papini<sup>25</sup>, A.V. Penacchioni<sup>29</sup>, B.F. Rauch<sup>32</sup>, S.B. Ricciarini<sup>25</sup>, K. Sakai<sup>3</sup>, T. Sakamoto<sup>1</sup>, M. Sasaki<sup>3</sup>, Y. Shimizu<sup>10</sup>, A. Shiomi<sup>17</sup>, R. Sparvoli<sup>28</sup>, P. Spillantini<sup>25</sup>, F. Stolzi<sup>29</sup>, I. Takahashi<sup>11</sup>, M. Takayanagi<sup>8</sup>, M. Takita<sup>7</sup>, T. Tamura<sup>10</sup>, N. Tateyama<sup>10</sup>, T. Terasawa<sup>7</sup>, H. Tomida<sup>8</sup>, S. Torii<sup>9,31</sup>, Y. Tunesada<sup>18</sup>, Y. Uchihori<sup>15</sup>, S. Ueno<sup>8</sup>, E. Vannuccini<sup>25</sup>, J.P. Wefel<sup>12</sup>, K. Yamaoka<sup>13</sup>, S. Yanagita<sup>6</sup>, A. Yoshida<sup>1</sup>, K. Yoshida<sup>21</sup>, and T. Yuda<sup>7</sup>

- 1) Aoyama Gakuin University, Japan
- 2) CRESST/NASA/GSFC and Universities Space Research Association, USA
- 3) CRESST/NASA/GSFC and University of Maryland, USA
- 4) Hirosaki University, Japan
- 5) Ibaraki National College of Technology, Japan
- 6) Ibaraki University, Japan
- 7) ICRR, University of Tokyo, Japan
- 8) ISAS/JAXA Japan
- 9) JAXA, Japan
- 10) Kanagawa University, Japan
- 11) Kavli IPMU, University of Tokyo, Japan
- 12) Louisiana State University, USA
- 13) Nagoya University, Japan
- 14) NASA/GSFC, USA
- 15) National Inst. of Radiological Sciences, Japan
- 16) National Institute of Polar Research, Japan
- 17) Nihon University, Japan

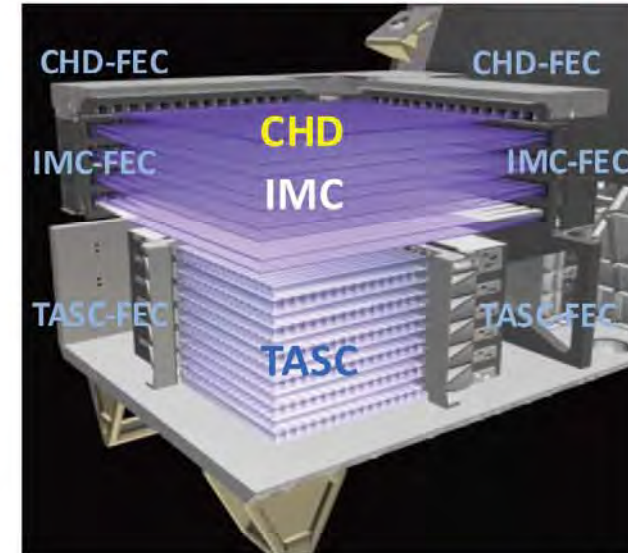
- 18) Osaka City University, Japan
- 19) Ritsumeikan University, Japan
- 20) Saitama University, Japan
- 21) Shibaura Institute of Technology, Japan
- 22) Shinshu University, Japan
- 23) St. Marianna University School of Medicine, Japan
- 24) University of Denver, USA
- 25) University of Florence, IFAC (CNR) and INFN, Italy
- 26) University of Padova and INFN, Italy
- 27) University of Pisa and INFN, Italy
- 28) University of Rome Tor Vergata and INFN, Italy
- 29) University of Siena and INFN, Italy
- 30) University of Tokyo, Japan
- 31) Waseda University, Japan
- 32) Washington University-St. Louis, USA
- 33) Yokohama National University, Japan
- 34) Yukawa Institute for Theoretical Physics, Kyoto University, Japan

# CALET System Overview

Launched Aug.2015



## CALORIMETER (CAL)



- **Mass:** 612.8 kg
- JEM Standard Payload Size  
1850mm(L) × 800mm(W) × 1000mm(H)
- **Power Consumption:** 507 W(max)
- **Telemetry:**  
Medium 600 kbps (6.5GB/day) / Low 50 kbps

(\* ) JEM stands for Japan Experiment Module

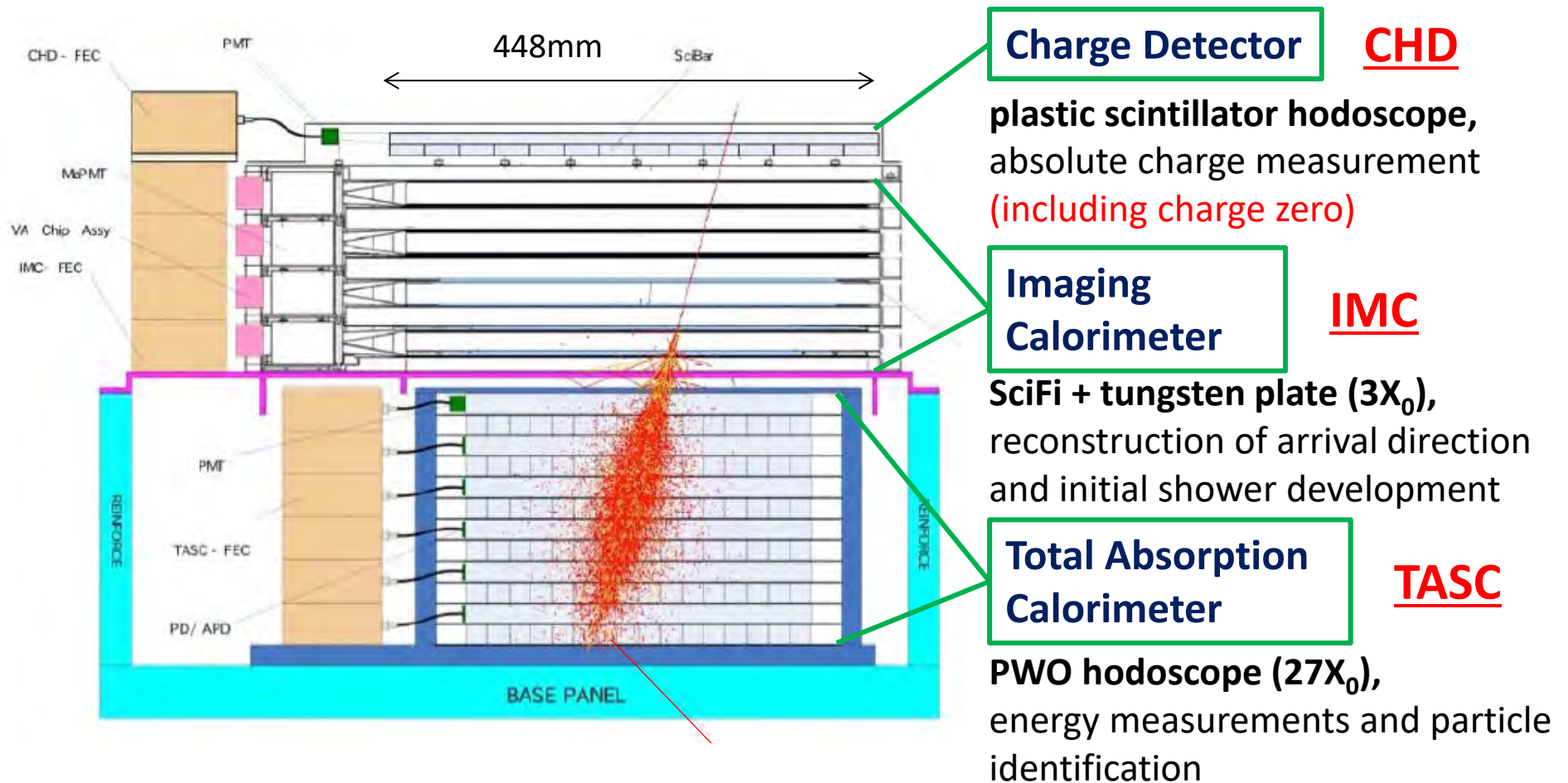
## CGBM (CALET Gamma-ray Burst Monitor)



# CALET-CAL Detector

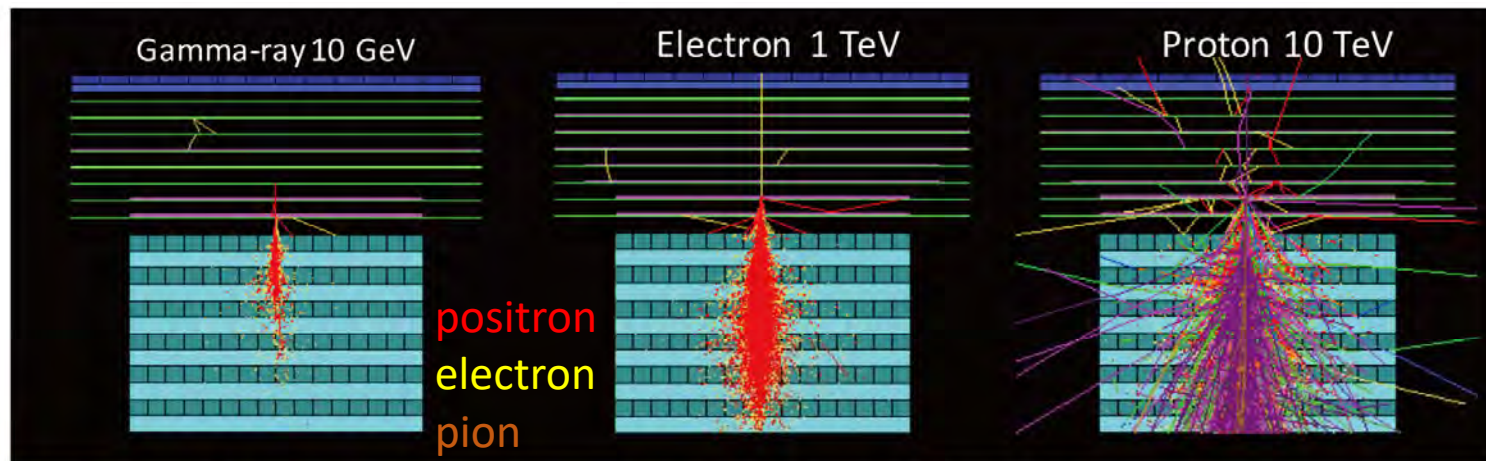


Fully active thick calorimeter ( $30X_0$ ) optimized for electron spectrum measurements well into TeV region

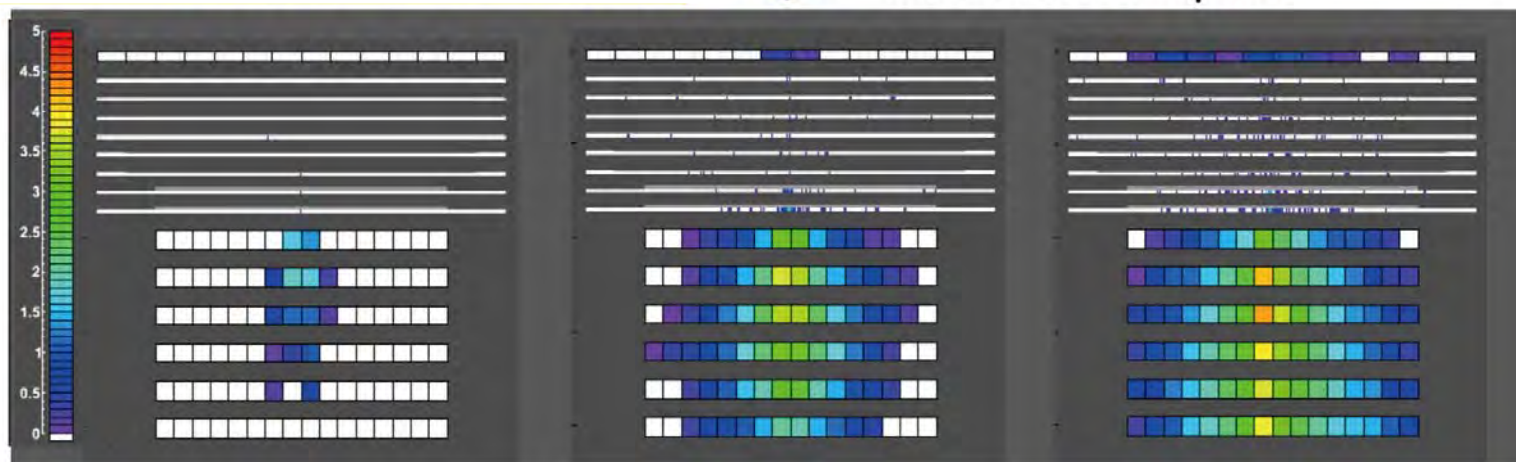


1TeV electron shower is fully contained in TASC

# CALET-CAL Shower Imaging Capability (MC)



In Detector Space



- Proton rejection power of  $10^5$  can be achieved by taking advantage of shower imaging capability of IMC and TASC
- Angular resolution of  $\sim 0.2^\circ$  for 10GeV gamma rays

# Overview of CALET Trigger System

Y. Asaoka et al., Astroparticle Phys. 100, 29 (2018)

**High Energy Shower  
Trigger (HE)**



- High energy electrons (10GeV ~20TeV)
- High energy gamma rays (10GeV ~10TeV)
- Nuclei (a few10GeV~1000TeV)

**Low Energy Shower  
Trigger (LE)**



- Low energy electron at high latitude (1GeV ~10GeV)
- GeV gamma-rays originated from GRB (1GeV ~)
- Ultra heavy nuclei (combined with heavy mode)

**Single Trigger (Single)**



- For detector calibration : penetrating particles  
(mainly non-interacting protons and heliums)

(\*) In addition to above 3 trigger modes, heavy modes are defined for each of the above trigger mode. They are omitted here for simple explanation.

**Auto Trigger  
(Pedestal/Test Pulse)**



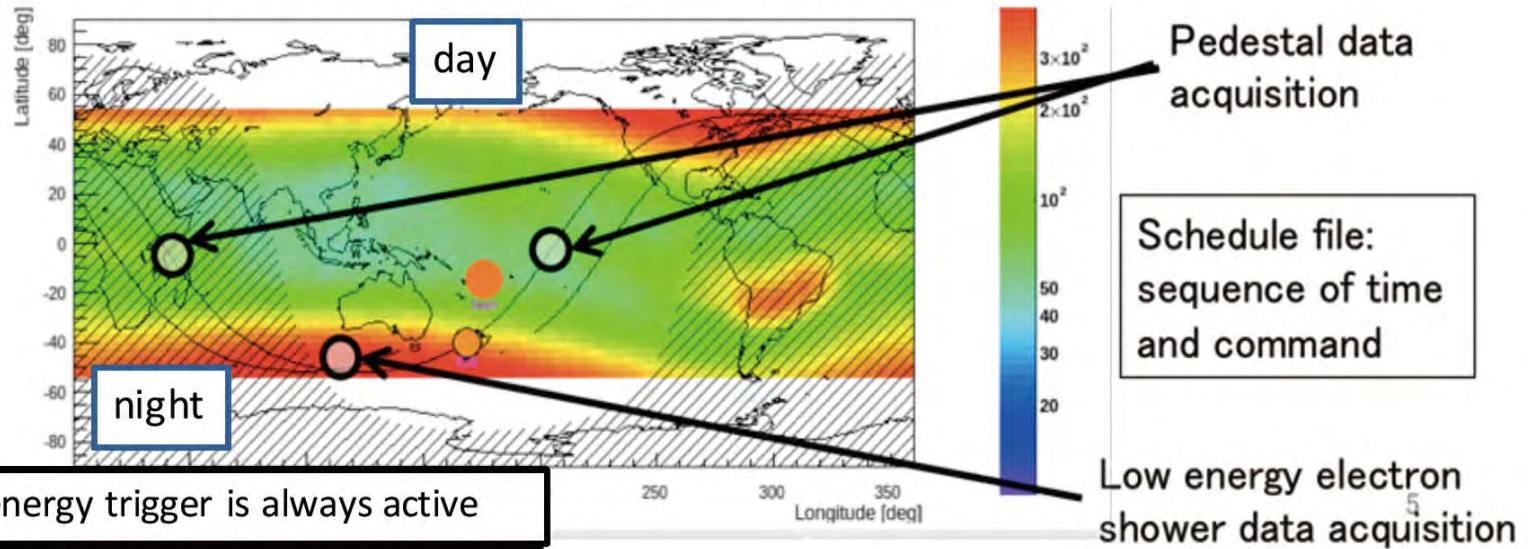
- For calibration:
  - ADC offset measurement (Pedestal)
  - FEC's response measurement (Test pulse)

# ISS Orbit and CALET Operations

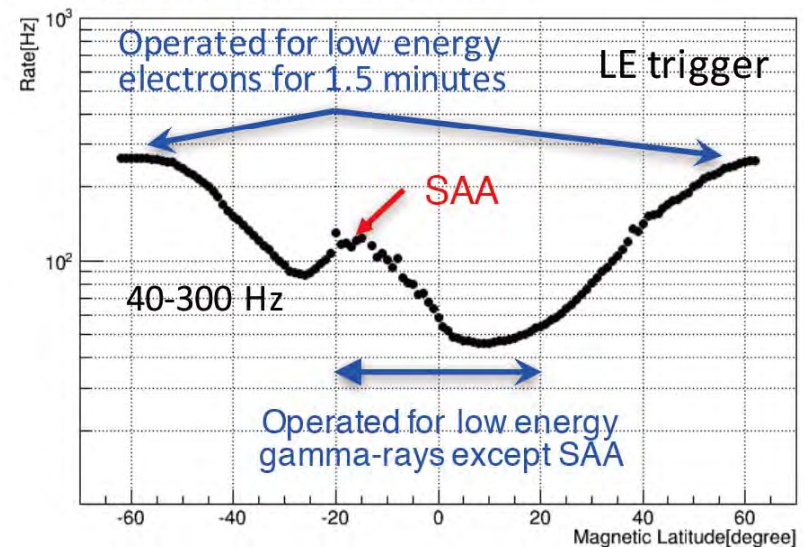
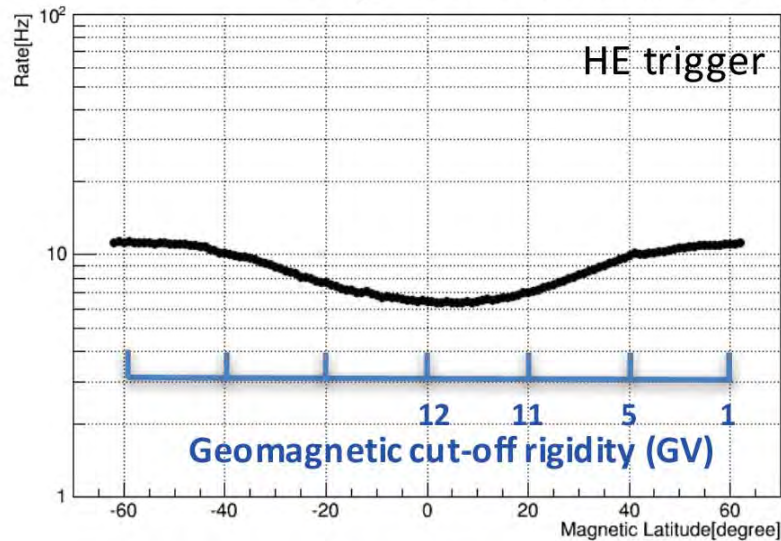
Y. Asaoka et al., Astroparticle Phys. 100, 29 (2018)

ISS orbit: inclination 51.6 degree, ~400 km

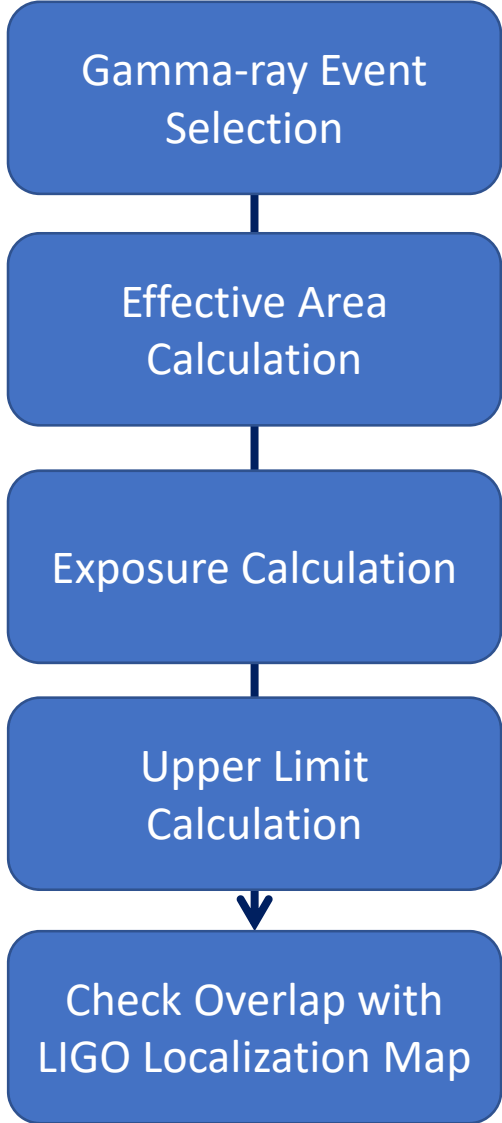
Concept of on-orbit operations



Dependence of the count rate on geomagnetic latitude



# CAL Limit Calculation Procedure



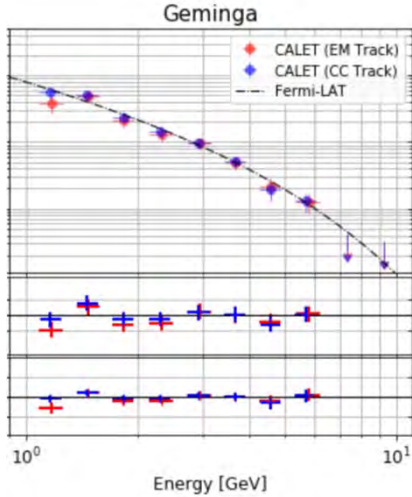
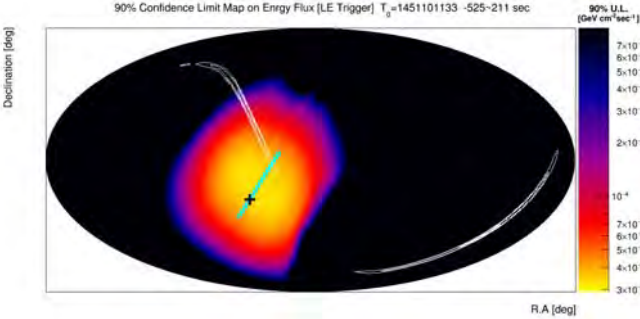
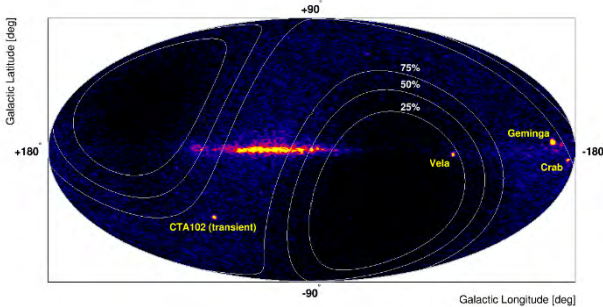
Lower energy is important

$S_{\text{eff}}$  as a function of zenith and azimuth

$S_{\text{eff}}(\text{zen}, \text{azi}) T_{\text{live}}$  projected to sky event by event along the ISS (CALET) orbit

**If no gamma-rays are observed**

Validation of Sensitivity with Observation of Diffuse/Point Sources





# Gamma Ray Event Selection

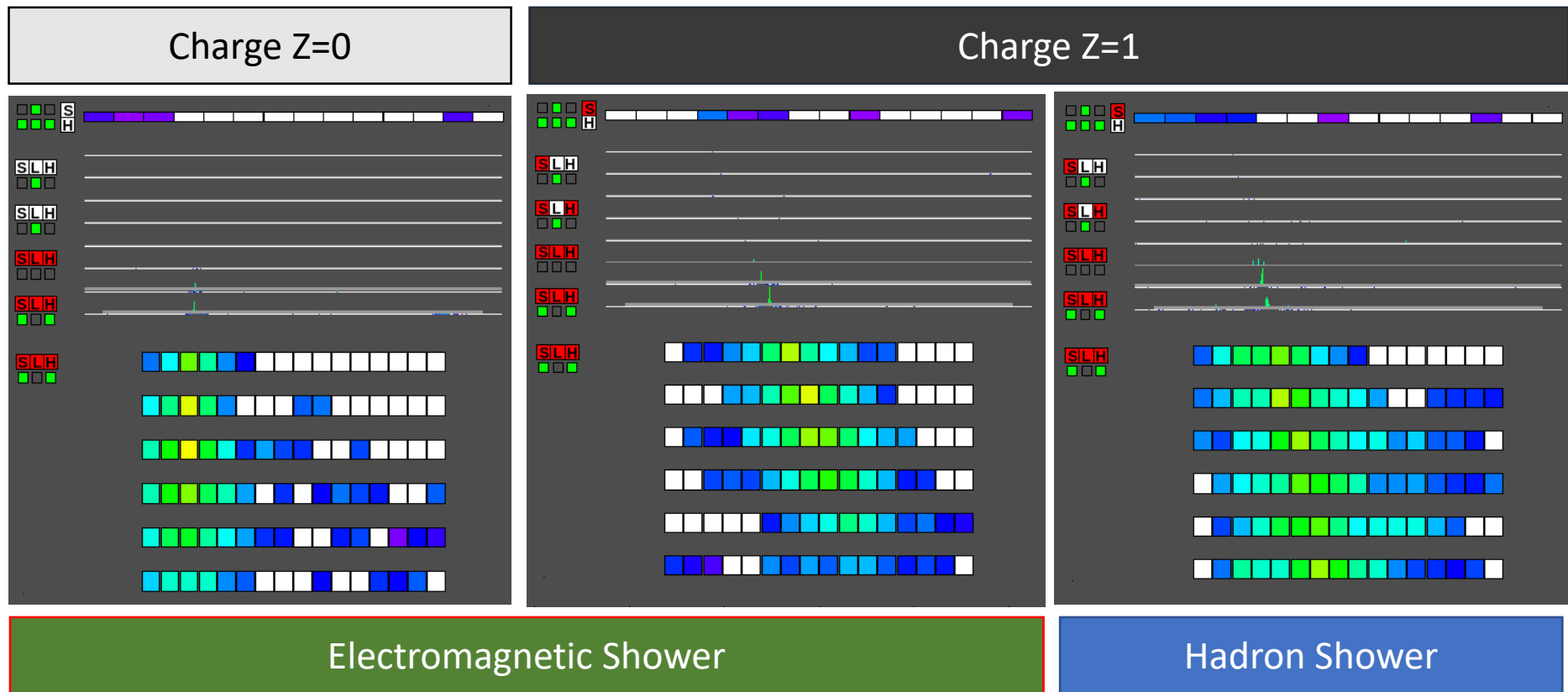
= Electron Selection Cut + Gamma-ray ID Cut w/ Lower Energy Extension

## 100 GeV Event Examples

gamma-ray

electron

proton

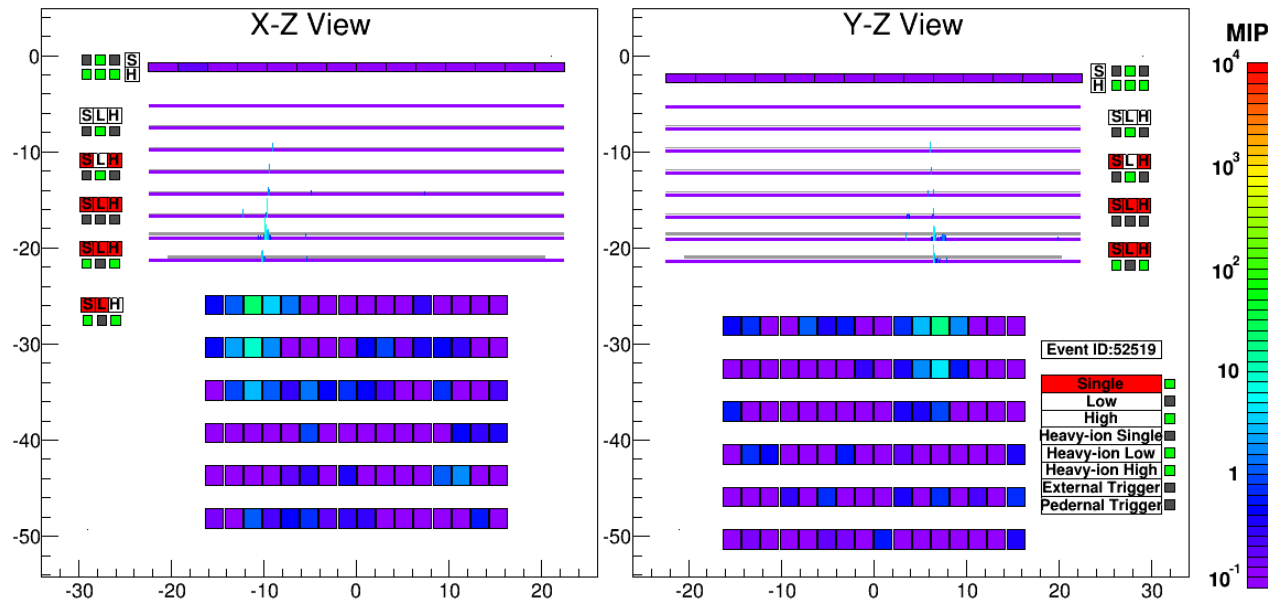


well contained, constant shower development

larger spread

# Gamma Ray Event Selection

= Electron Selection Cut + Gamma-ray ID Cut w/ Lower Energy Extension

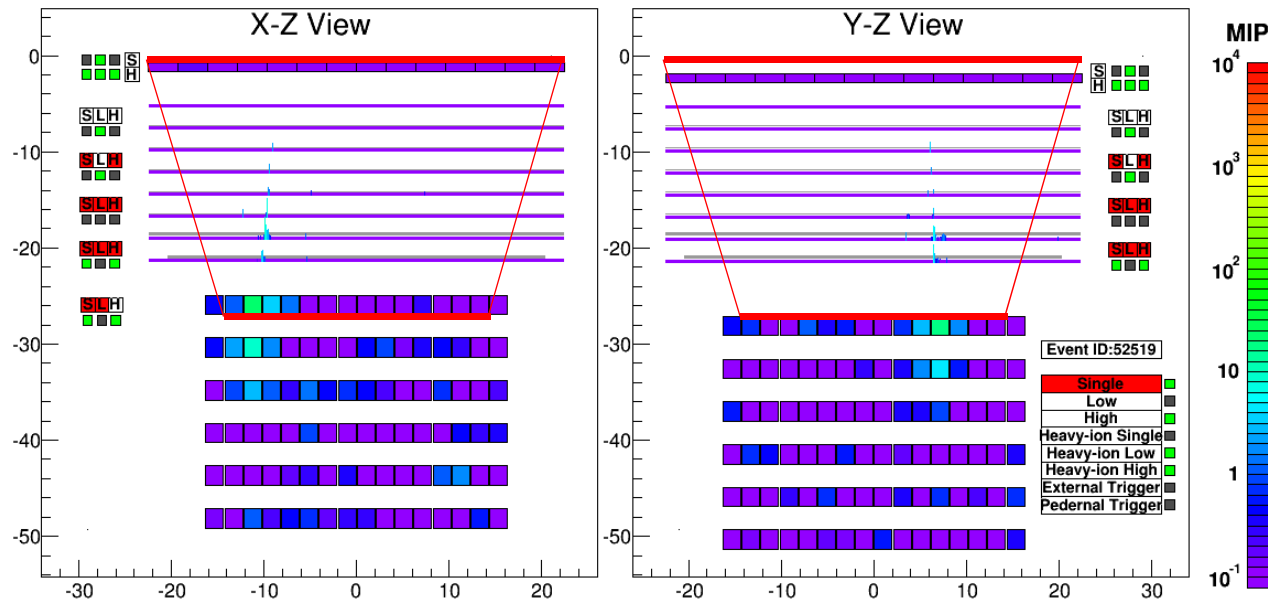


An example of gamma-ray event candidate in flight data  
(reconstructed primary energy  $\sim 5\text{GeV}$ )

1. Geometry Condition
  - CHD-Top to TASC  
1<sup>st</sup> layer (2cm margin)
2. Pre selection
  - Offline trigger
  - Shower concentration
  - Shower starting point
3. Track quality cut
  - Track hits  $> 2$
  - matching w/ TASC
4. Electromagnetic shower selection
  - shower shape
5. Gamma-ray ID
  - CHD/IMC-veto  
(combination of loose cuts)
6. FOV cut

# Gamma Ray Event Selection

= Electron Selection Cut + Gamma-ray ID Cut w/ Lower Energy Extension



To maximize the field of view (FOV), the requirements on acceptance condition was loosened as much as possible compared to electron analysis. However, penetration of CHD paddle by shower axis is required to ensure charge zero selection.

1. Geometry Condition
  - CHD-Top to TASC
  - 1<sup>st</sup> layer (2cm margin)
2. Pre selection
  - Offline trigger
  - Shower concentration
  - Shower starting point
3. Track quality cut
  - Track hits >2
  - matching w/ TASC
4. Electromagnetic shower selection
  - shower shape
5. Gamma-ray ID
  - CHD/IMC-veto (combination of loose cuts)
6. FOV cut

# Gamma Ray Event Selection

= Electron Selection Cut + Gamma-ray ID Cut w/ Lower Energy Extension

“K-cut” 
$$K = \log_{10}(F_E) + \frac{1}{2}R_E$$

$F_E$ : fractional energy deposit of TASC-Y6 relative to total TASC deposit

$R_E$ : second moment of lateral energy deposit distribution relative to shower axis [cm]

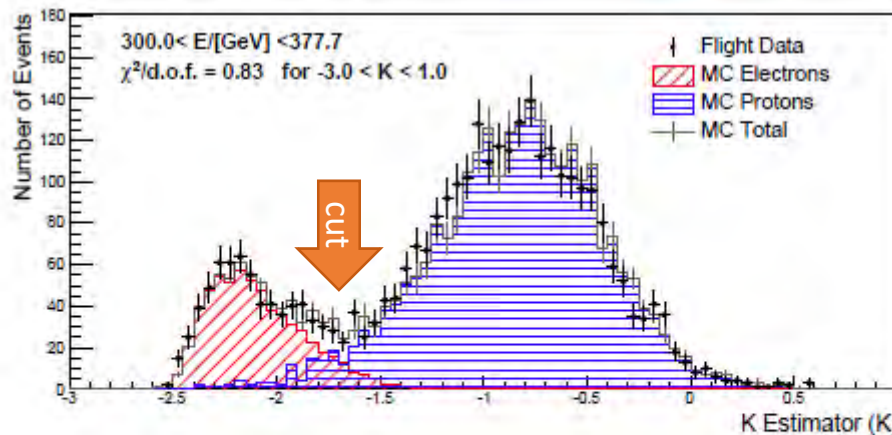


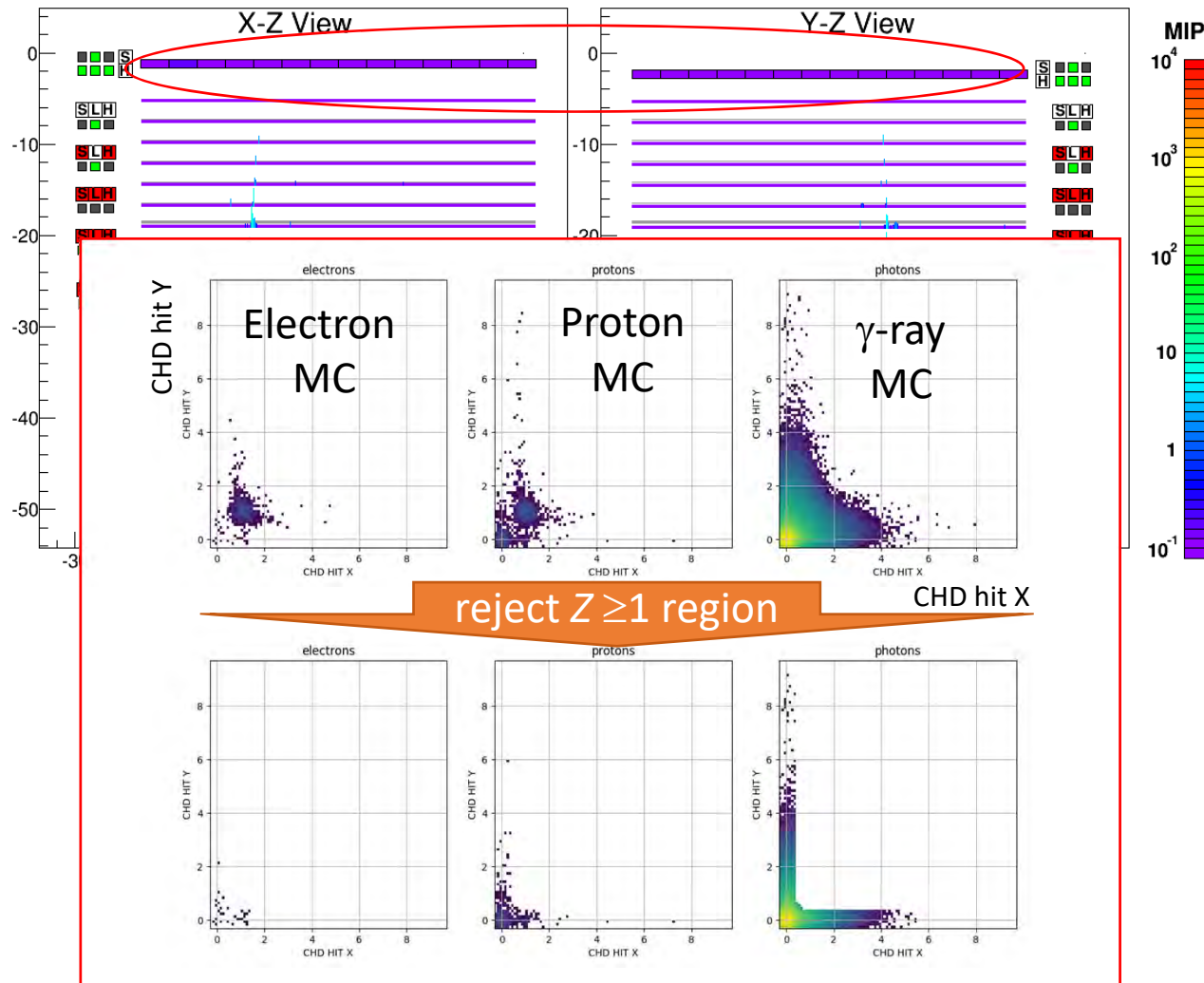
FIG. 2. An example of K-estimator distribution in the  $300 < E < 378$  GeV bin. The reduced chi-square of the fit in the K-estimator range from -3 to 1 is 0.83.

O. Adriani et al., PRL 119, 181101 (2017) supplemental material

1. Geometry Condition
  - CHD-Top to TASC 1<sup>st</sup> layer (2cm margin)
2. Pre selection
  - Offline trigger
  - Shower concentration
  - Shower starting point
3. Track quality cut
  - Track hits >2
  - matching w/ TASC
4. Electromagnetic shower selection
  - shower shape
5. Gamma-ray ID
  - CHD/IMC-veto (combination of loose cuts)
6. FOV cut

# Gamma Ray Event Selection

= Electron Selection Cut + Gamma-ray ID Cut w/ Lower Energy Extension

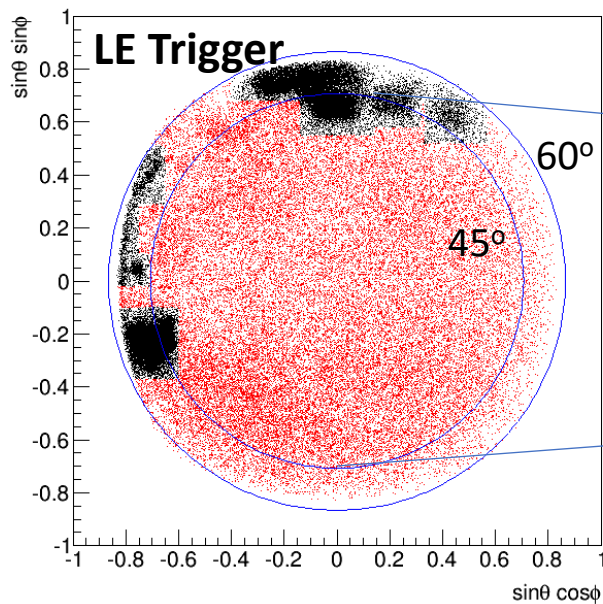


1. Geometry Condition
  - CHD-Top to TASC
  - 1<sup>st</sup> layer (2cm margin)
2. Pre selection
  - Offline trigger
  - Shower concentration
  - Shower starting point
3. Track quality cut
  - Track hits >2
  - matching w/ TASC
4. Electromagnetic shower selection
  - shower shape
5. Gamma-ray ID
  - CHD/IMC-veto
  - (combination of loose cuts)
6. FOV cut

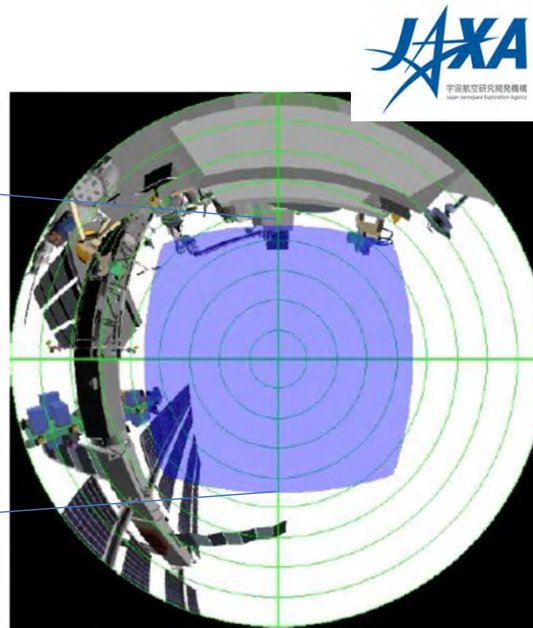
# Gamma Ray Event Selection

= Electron Selection Cut + Gamma-ray ID Cut w/ Lower Energy Extension

It was found that secondary gamma-ray produced in ISS structures are dominant source of background



Gamma-ray candidates in CALET FOV



Fish-eye view of CALET FOV

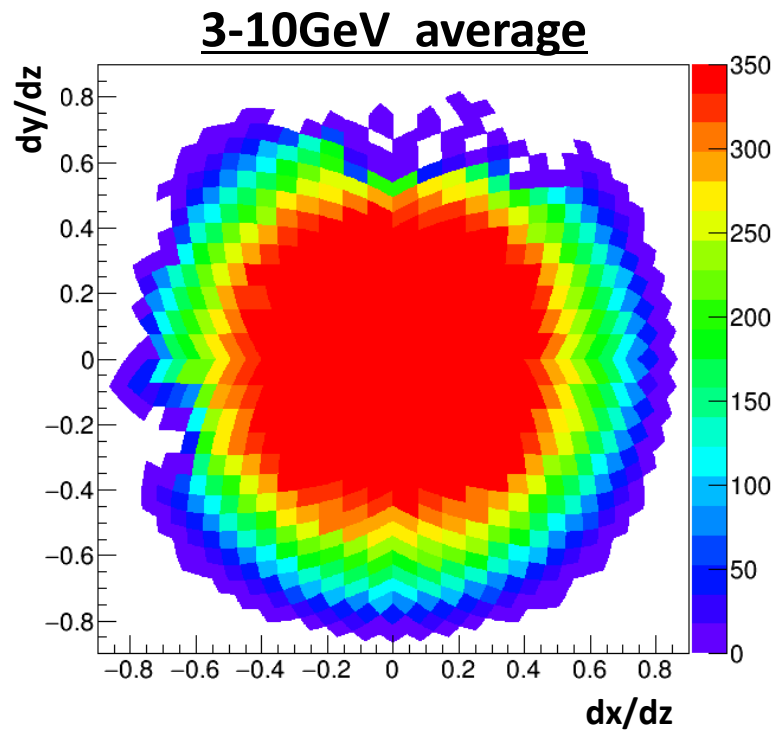
By removing Black parts, it is possible to reject majority of such background. More sophisticated rejection method is under development.

1. Geometry Condition
  - CHD-Top to TASC
  - 1<sup>st</sup> layer (2cm margin)
2. Pre selection
  - Offline trigger
  - Shower concentration
  - Shower starting point
3. Track quality cut
  - Track hits >2
  - matching w/ TASC
4. Electromagnetic shower selection
  - shower shape
5. Gamma-ray ID
  - CHD-veto
6. FOV cut

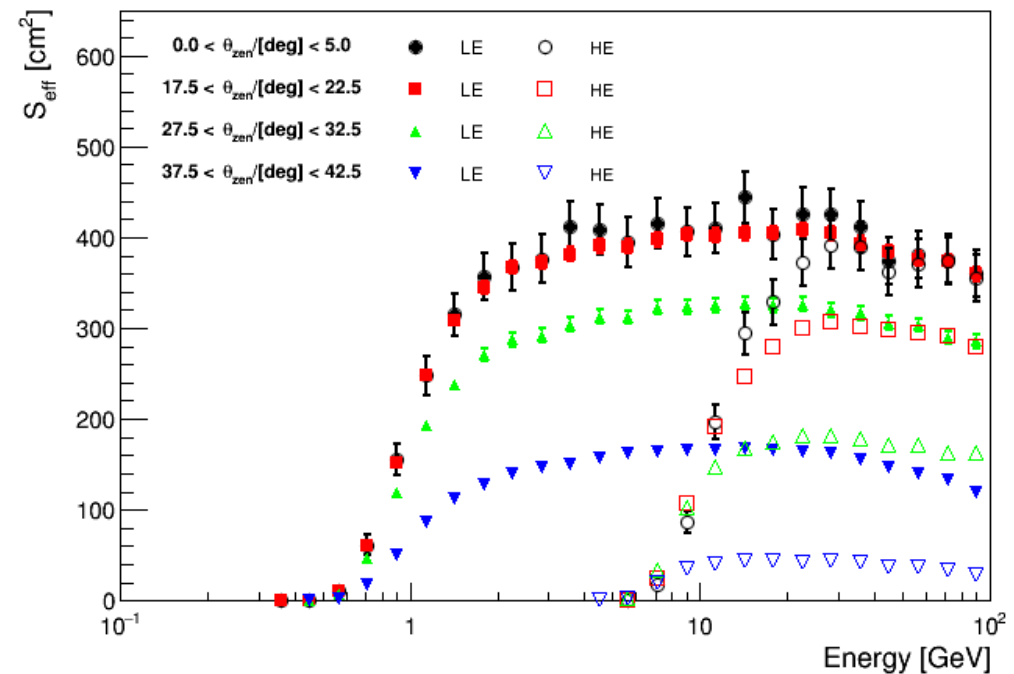
# Effective Area and Sensitivity

Preliminary  
O. Adriani et al., in prep.

Effective area is estimated as a function of incident angle ( $dx/dz$ ,  $dy/dz$ ) and energy.  
Maximum effective area is achieved at around 5 GeV, but lower energy is more important for steep spectrum like  $E^{-2}$ .



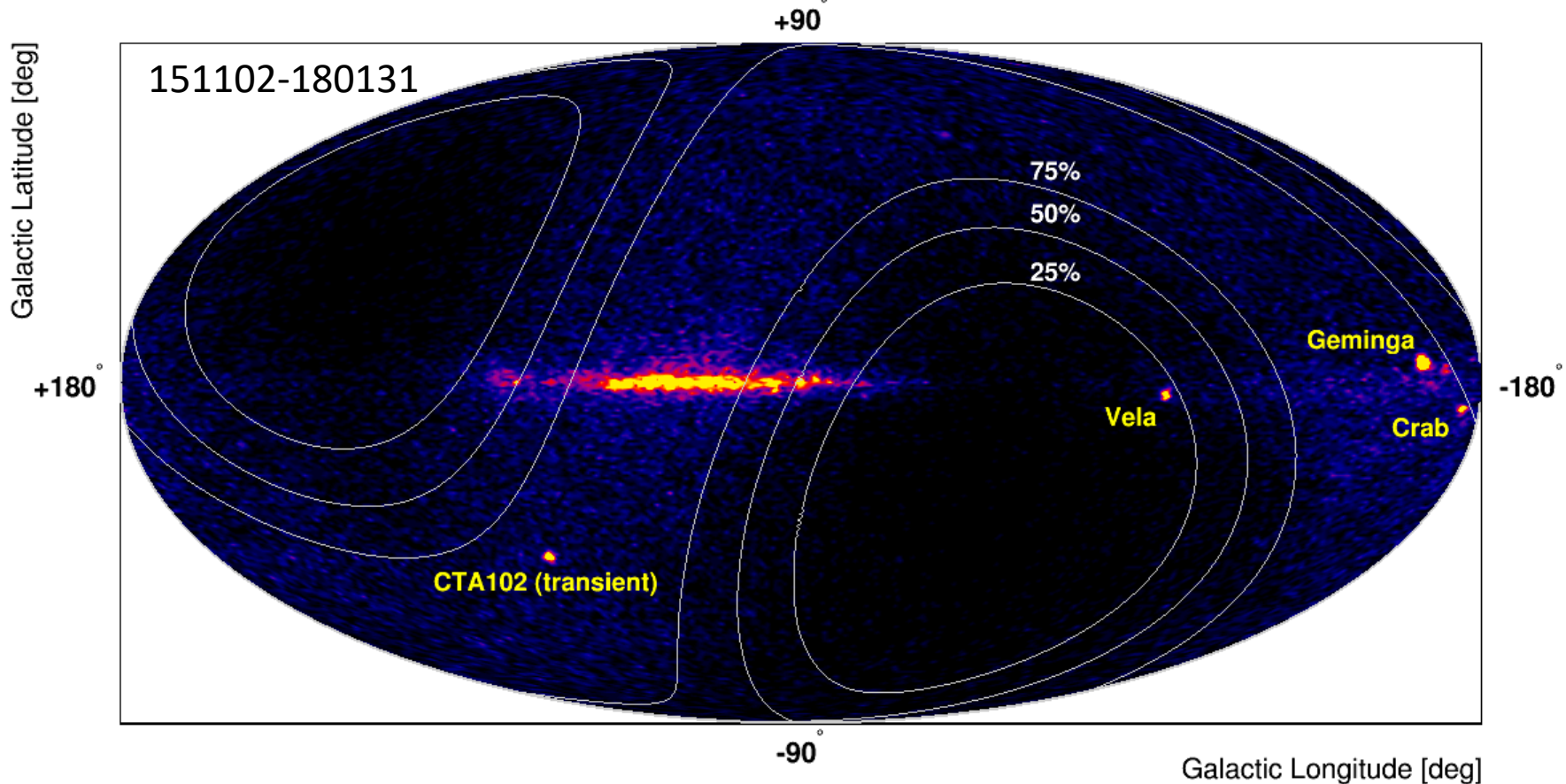
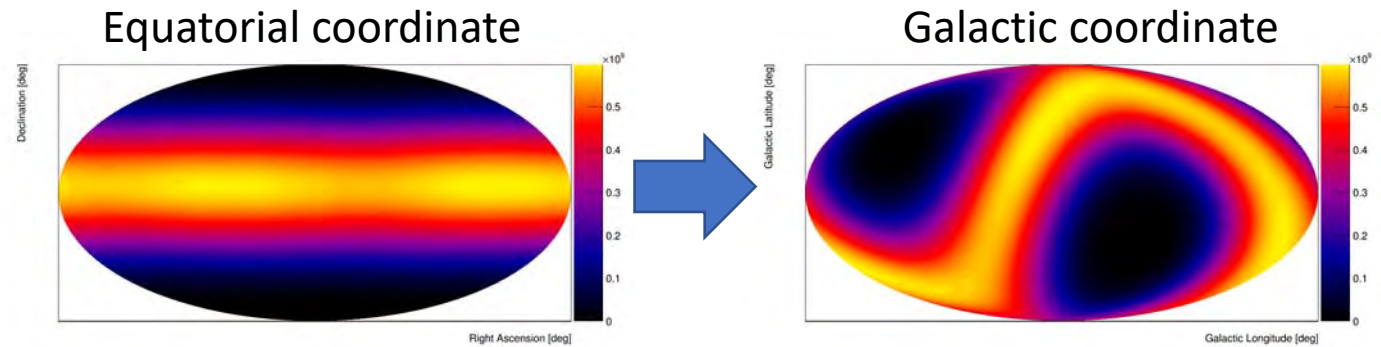
Mostly axially symmetric except for FOV cut



Effective area as a function of energy. Four representing zenith angle ranges are shown.

# CALET Sky Map w/ LE- $\gamma$ Trigger ( $E > 1\text{GeV}$ )

While exposure is not uniform, we have clearly identified the galactic plane and bright GeV sources.

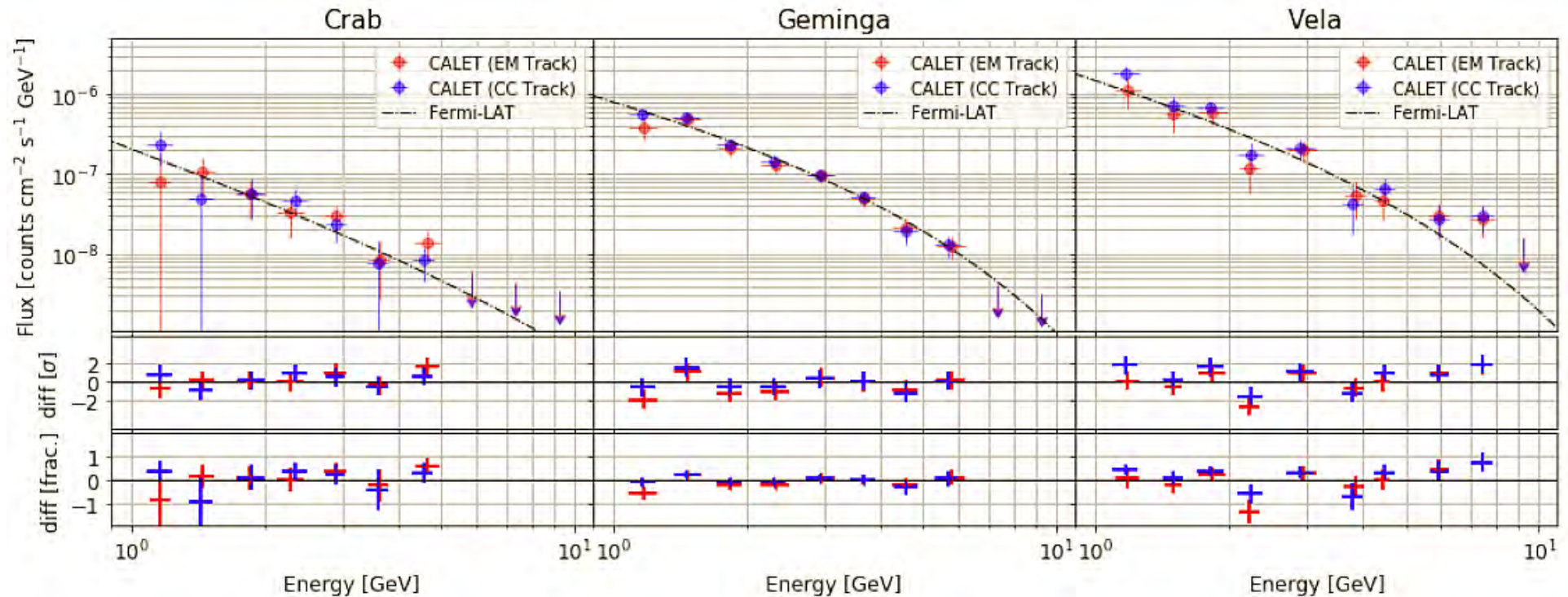




# Point Source Spectra: Sensitivity Validation

## CALET Preliminary

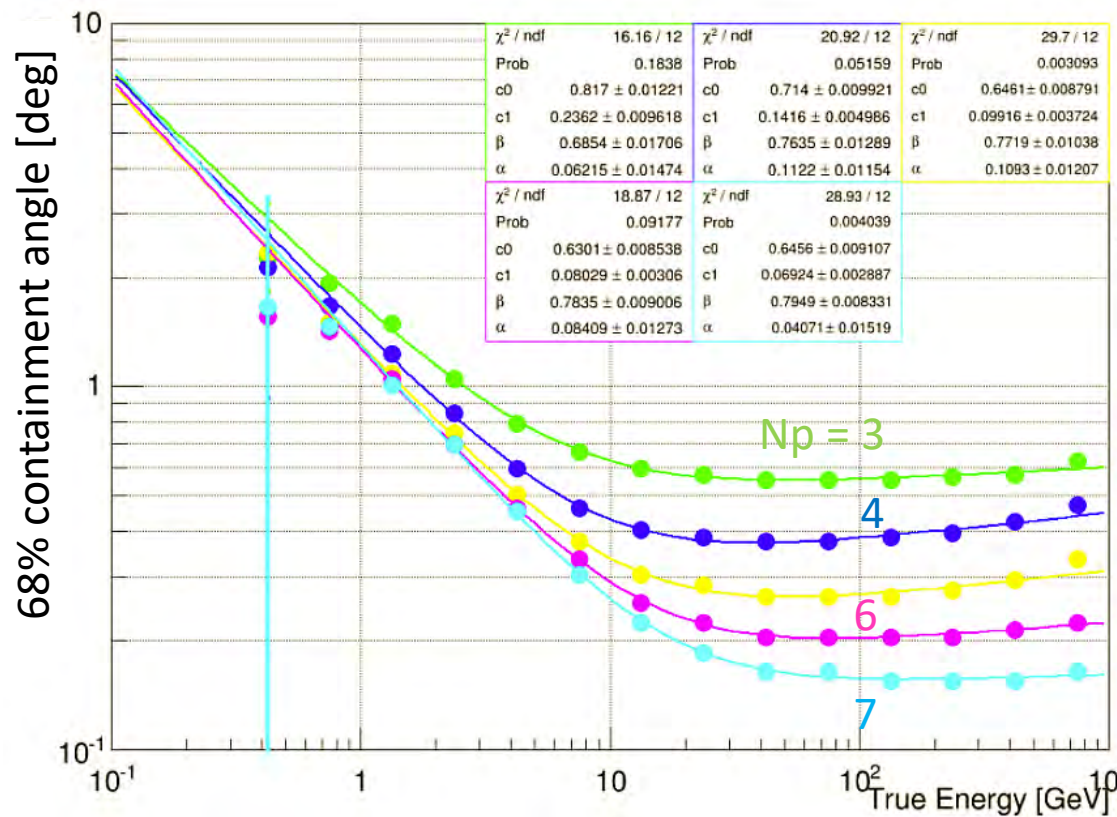
N. Cannady et al., in prep.



Fermi-LAT's parameterizations. Therefore, it was found that current selection criteria has a validated sensitivity and can be used to set limit on GW counterpart flux.

# Angular resolution

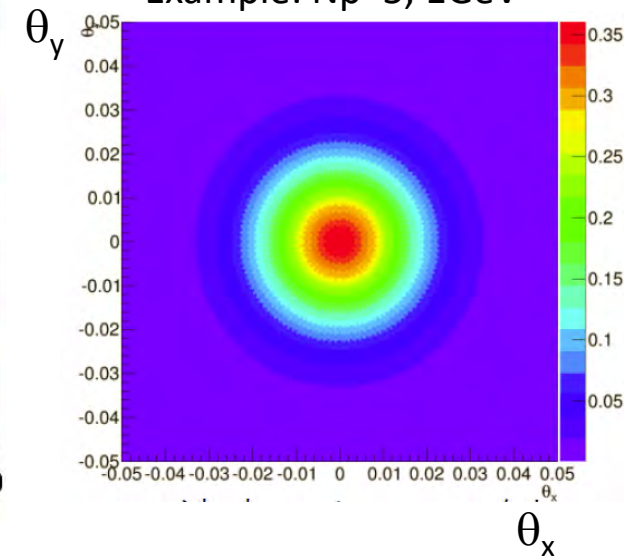
- Containment angles by Monte Carlo simulation



$$S_p(E, N_p) = \sqrt{(c_0 E^{-\beta})^2 + c_1^2 \times (1 + E^\delta)}$$

$N_p$  : number of points used for track reconstruction

Example:  $N_p=5, 1\text{GeV}$



# Gravitational-wave events by LIGO/Virgo

**Table 1.** List of gravitational-wave events reported by the Virgo and LIGO scientific collaborations and summary of inferred parameters (at the 90% credible level). (BH: black hole, NS: neutron star)

GW event	Time (UTC)	Location area (deg <sup>2</sup> )	Luminosity distance (Mpc)	Energy radiated ( $M_{\odot}c^2$ )	Primary		Secondary		Remnant		Ref.	
					Type	Mass ( $M_{\odot}$ )	Type	Mass ( $M_{\odot}$ )	Type	Mass ( $M_{\odot}$ )		
CALET ↓	GW150914	2015-09-14 09:50:45	230	$420^{+150}_{-180}$	$3.0^{+0.5}_{-0.4}$	BH	$36.2^{+5.2}_{-3.8}$	BH	$29.1^{+3.7}_{-4.4}$	BH	$62.3^{+3.7}_{-3.1}$	Abbott et al. (2016d)
	GW151226	2015-12-26 09:54:43	850	$440^{+180}_{-190}$	$1.0^{+0.1}_{-0.2}$	BH	$14.2^{+8.3}_{-3.7}$	BH	$7.5^{+2.3}_{-2.3}$	BH	$20.8^{+6.1}_{-1.7}$	Abbott et al. (2016c)
	GW170104	2017-01-04 10:11:58	1200	$880^{+450}_{-390}$	$2.0^{+0.6}_{-0.7}$	BH	$31.2^{+8.4}_{-6.0}$	BH	$19.4^{+5.3}_{-5.9}$	BH	$48.7^{+5.7}_{-4.6}$	Abbott et al. (2017a)
	GW170608	2017-06-08 02:01:16	520	$340^{+140}_{-140}$	$0.85^{+0.07}_{-0.17}$	BH	$12^{+7}_{-5}$	BH	$7^{+2}_{-2}$	BH	$18.0^{+4.8}_{-0.9}$	Abbott et al. (2017f)
	GW170814	2017-08-14 10:30:43	60	$540^{+130}_{-210}$	$2.7^{+0.4}_{-0.3}$	BH	$30.5^{+5.7}_{-3.0}$	BH	$25.3^{+2.8}_{-4.2}$	BH	$53.2^{+3.2}_{-2.5}$	Abbott et al. (2017b)
	GW170817	2017-08-17 12:41:04	28	$40^{+8}_{-14}$	$> 0.025$	NS	1.36–1.60	NS	1.17–1.36	NS	$2.74^{+0.04}_{-0.01}$	Abbott et al. (2017c) or BH

# GW Counterpart Search with CALET

THE ASTROPHYSICAL JOURNAL LETTERS, 829:L20 (5pp), 2016 September 20  
© 2016. The American Astronomical Society. All rights reserved.

doi:10.3847/2041-8205/829/1/L20



## CALET UPPER LIMITS ON X-RAY AND GAMMA-RAY COUNTERPARTS OF GW151226

O. ADRIANI<sup>1,2,3</sup>, Y. AKAIKE<sup>4,5</sup>, K. ASANO<sup>6</sup>, Y. ASAOKA<sup>7,8</sup>, M. G. BAGLIESI<sup>2,9</sup>, G. BIGONGIARI<sup>2,9</sup>, W. R. BINNS<sup>10</sup>, S. BONECHI<sup>2,9</sup>, M. BONGI<sup>1,2,3</sup>, P. BROGI<sup>2,9</sup>, J. H. BUCKLEY<sup>10</sup>, N. CANNADY<sup>11</sup>, G. CASTELLINI<sup>1,2,3</sup>, C. CHECCHIA<sup>12</sup>, M. L. CHERRY<sup>11</sup>, G. COLLAZUOL<sup>12</sup>, V. DI FELICE<sup>2,13</sup>, K. EBISAWA<sup>14</sup>, H. FUKU<sup>14</sup>, T. G. GUZIK<sup>11</sup>, T. HAMS<sup>5,15</sup>, M. HAREYAMA<sup>16</sup>, N. HASEBE<sup>8</sup>, K. HIBINO<sup>17</sup>, M. ICHIMURA<sup>18</sup>, K. IOKA<sup>19</sup>, W. ISHIZAKI<sup>6</sup>, M. H. ISRAEL<sup>10</sup>, A. JAVAD<sup>11</sup>, K. KASAHARA<sup>8</sup>, J. KATAOKA<sup>8</sup>, R. KATAOKA<sup>20</sup>, Y. KATAYOSE<sup>21</sup>, C. KATO<sup>22</sup>, N. KAWANAKA<sup>23</sup>, Y. KAWAKUBO<sup>24</sup>, H. KITAMURA<sup>25</sup>, H. S. KRAWCZYNSKI<sup>10</sup>, J. F. KRIZMANIC<sup>4,5</sup>, S. KURAMATA<sup>18</sup>, T. LOMTADZE<sup>26</sup>, P. MAESTRO<sup>2,9</sup>, P. S. MARROCCHESI<sup>2,9</sup>, A. M. MESSINEO<sup>26</sup>, J. W. MITCHELL<sup>27</sup>, S. MIYAKE<sup>28</sup>, K. MIZUTANI<sup>29</sup>, A. A. MOISEEV<sup>5,30</sup>, K. MORI<sup>8,14</sup>, M. MORI<sup>31</sup>, N. MORI<sup>1,2,3</sup>, H. M. MOTZ<sup>32</sup>, K. MUNAKATA<sup>22</sup>, H. MURAKAMI<sup>8</sup>, Y. E. NAKAGAWA<sup>14</sup>, S. NAKAHIRA<sup>7</sup>, J. NISHIMURA<sup>14</sup>, S. OKUNO<sup>17</sup>, J. F. ORMES<sup>33</sup>, S. OZAWA<sup>8</sup>, L. PACINI<sup>1,2,3</sup>, F. PALMA<sup>2,13</sup>, P. PAPINI<sup>1,2,3</sup>, A. V. PENACCHIONI<sup>9,34</sup>, B. F. RAUCH<sup>10</sup>, S. RICCIARINI<sup>1,2,3</sup>, K. SAKAI<sup>5,15</sup>, T. SAKAMOTO<sup>24</sup>, M. SASAKI<sup>5,30</sup>, Y. SHIMIZU<sup>17</sup>, A. SHIOMI<sup>35</sup>, R. SPARVOLI<sup>2,13</sup>, P. SPILLANTINI<sup>1,2,3</sup>, F. STOLZI<sup>2,9</sup>, I. TAKAHASHI<sup>36</sup>, M. TAKAYANAGI<sup>14</sup>, M. TAKITA<sup>6</sup>, T. TAMURA<sup>17</sup>, N. TATEYAMA<sup>17</sup>, T. TERASAWA<sup>37</sup>, H. TOMIDA<sup>14</sup>, S. TORII<sup>7,8</sup>, Y. TSUNESADA<sup>38</sup>, Y. UCHIHORI<sup>25</sup>, S. UENO<sup>14</sup>,

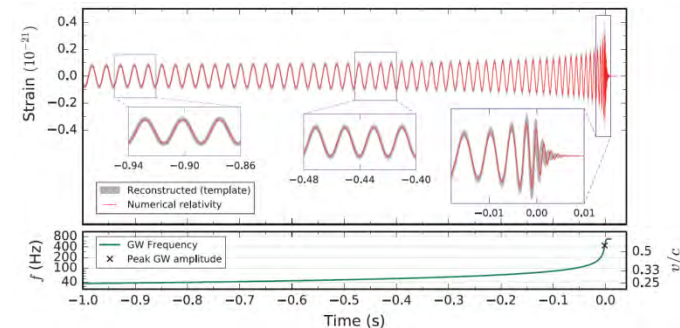
Published  
in ApJ Letters

## GW 151226 [B. P. Abbott *et al.*, PRL 116 (2016) 241103]

- GW trigger Time: 2015/12/26 3:38:53.647 UT
  - **gravitational-wave signal** produced by the coalescence of two stellar-mass black holes at a luminosity distance of  $\sim 440$ Mpc.

## CALET Observation

- CGBM HV-on (3:20 – 3:40 UT)
  - No on-board trigger
- **CAL: low-energy gamma-ray mode ( $> 1$ GeV) 3:30-3:43UT**



# Analysis update

- EM Track ... developed and used extensively for electron analysis
- **CC Track** ... developed specifically for low energy gamma-rays

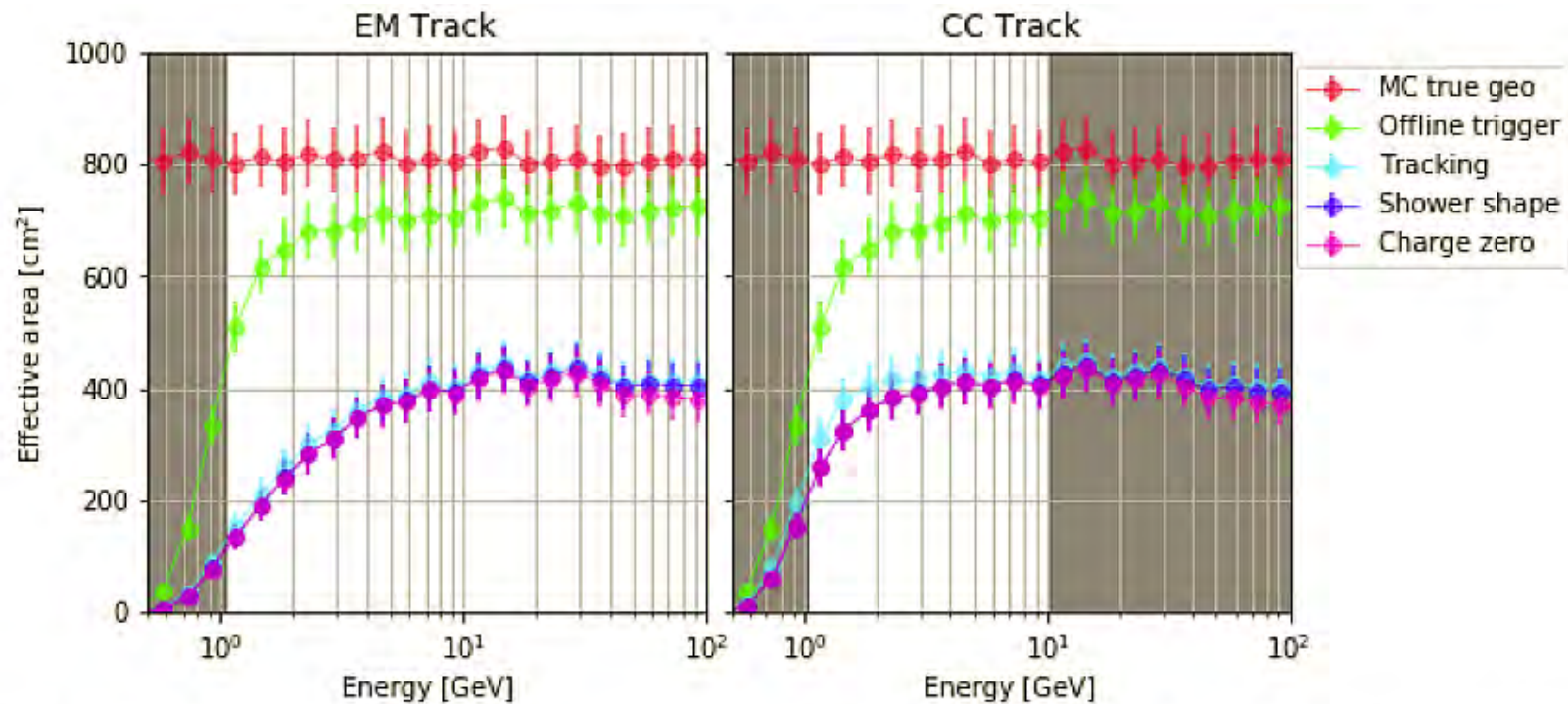


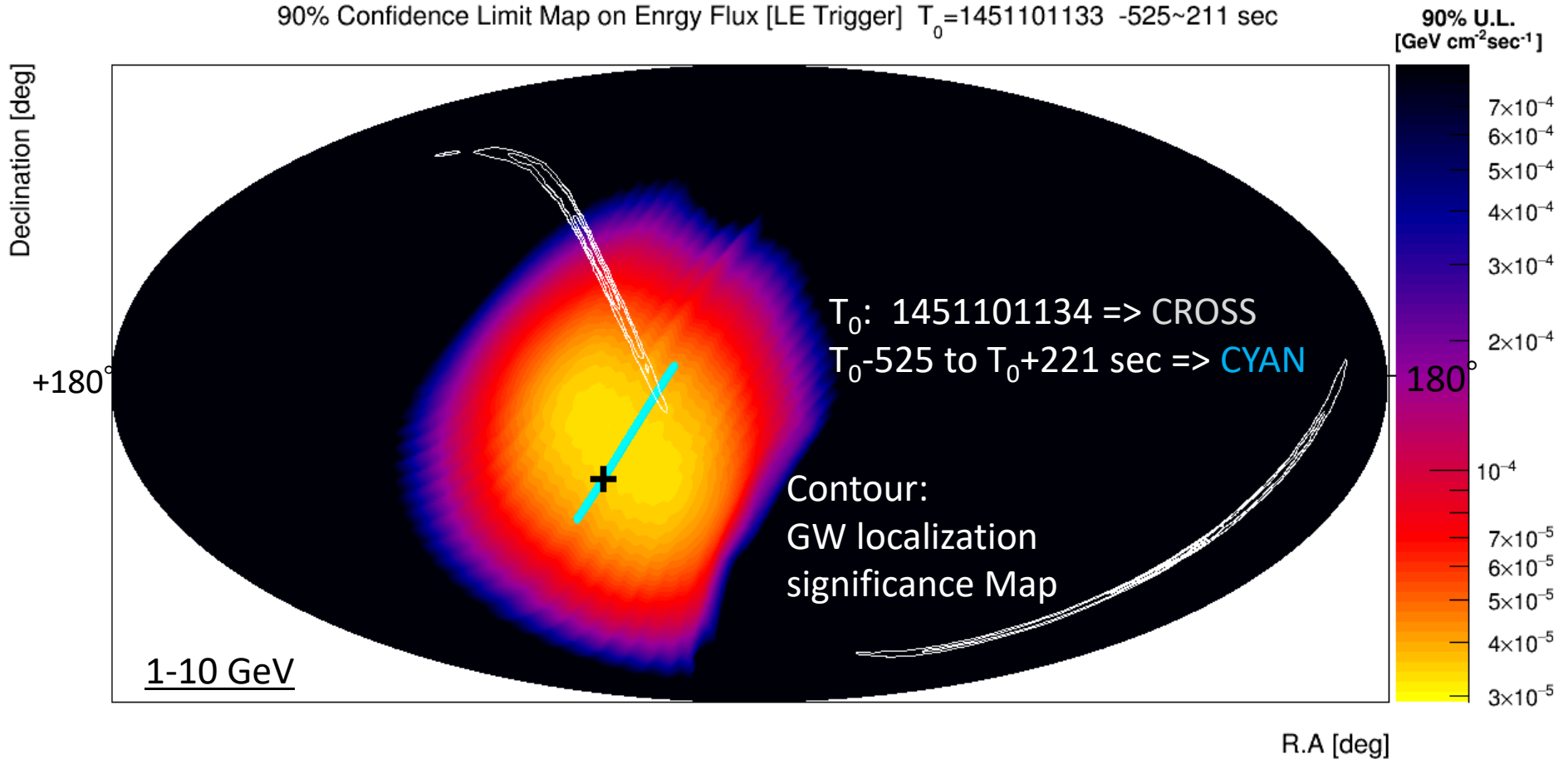
Figure 3. Effect of various selection cuts in zenith-pointing effective area. Grey shaded regions demonstrate the limits of applicability for each track due to background contamination with poor agreement between flight data and simulation.

# 90% CL Upper limit for GW151226 Counterpart Search

Preliminary  
O. Adriani et al., in prep.

**NO event remained after applying all the selection criteria.**

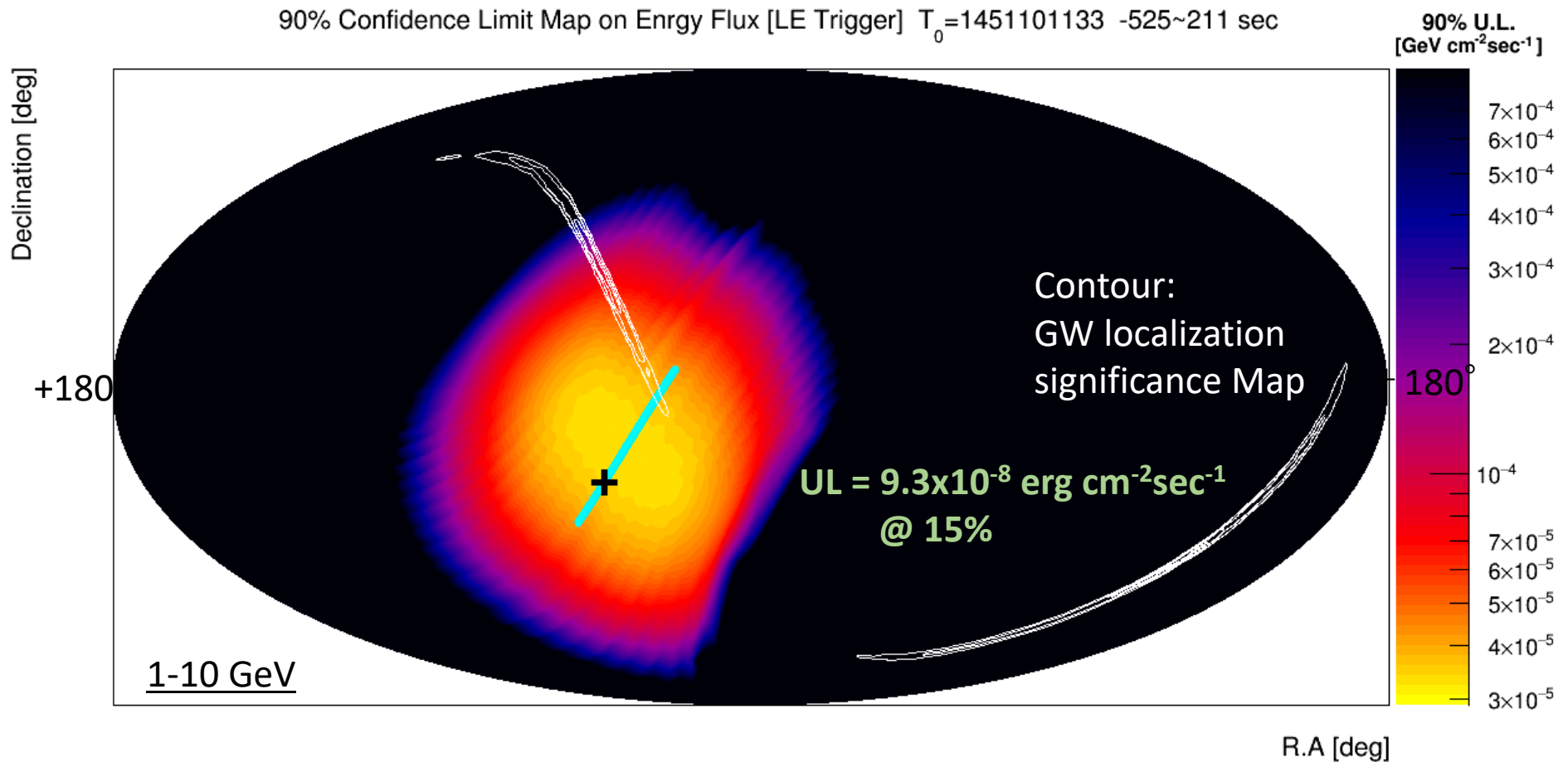
90% Confidence Limit Map on Enrgy Flux [LE Trigger]  $T_0=1451101133$  -525~211 sec



**Background contamination is negligible in such a short time period.**

# 90% CL Upper limit for GW151226 counterpart search

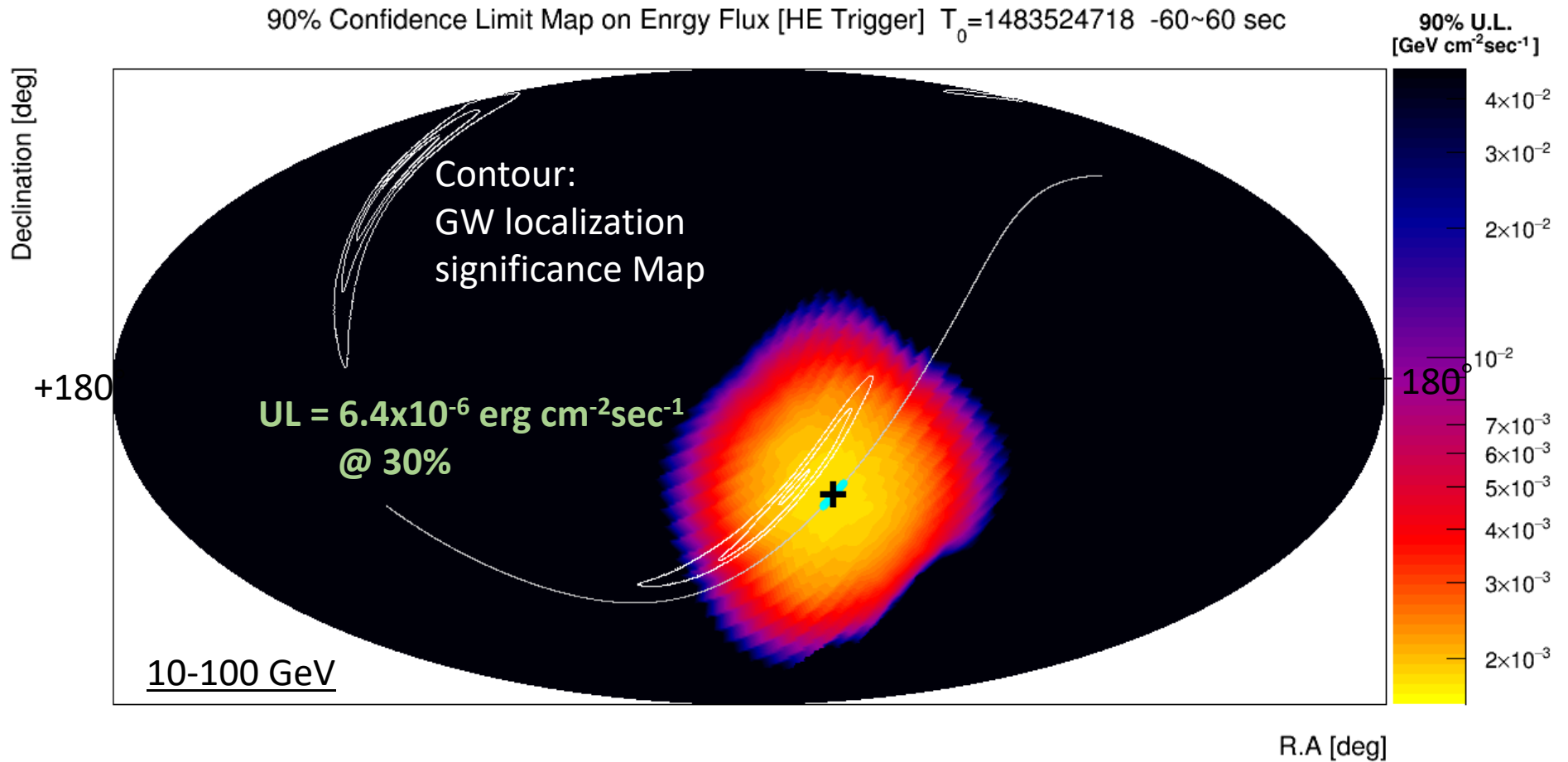
Preliminary  
O. Adriani et al., in prep.



CALET observation constrains at least some portion of LIGO probability.

# 90% CL Upper limit for GW170104 counterpart search

Preliminary  
O. Adriani et al., in prep.

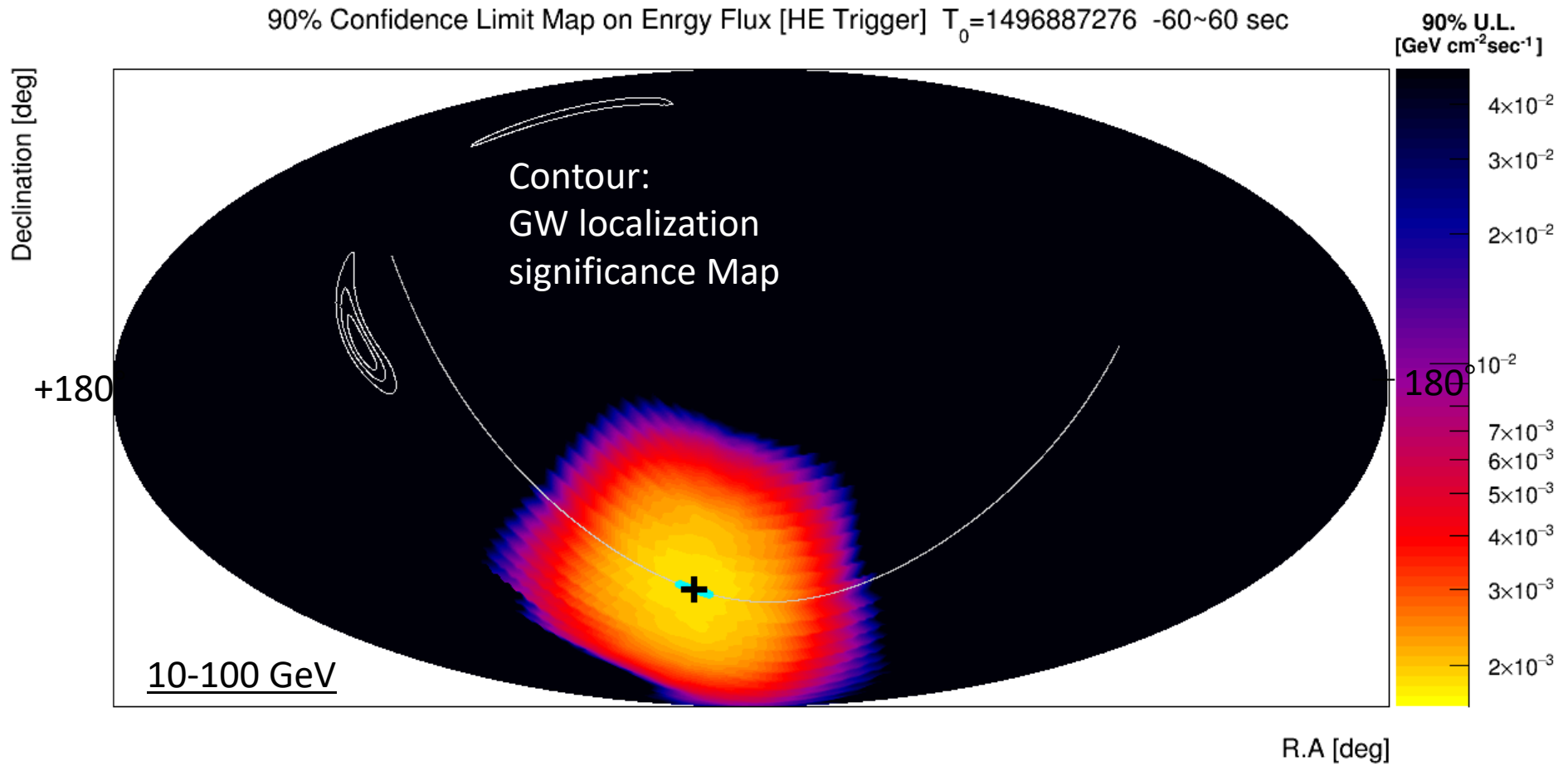


CALET observation constrains at least some portion of LIGO probability.



# 90% CL Upper limit for GW170608 counterpart search

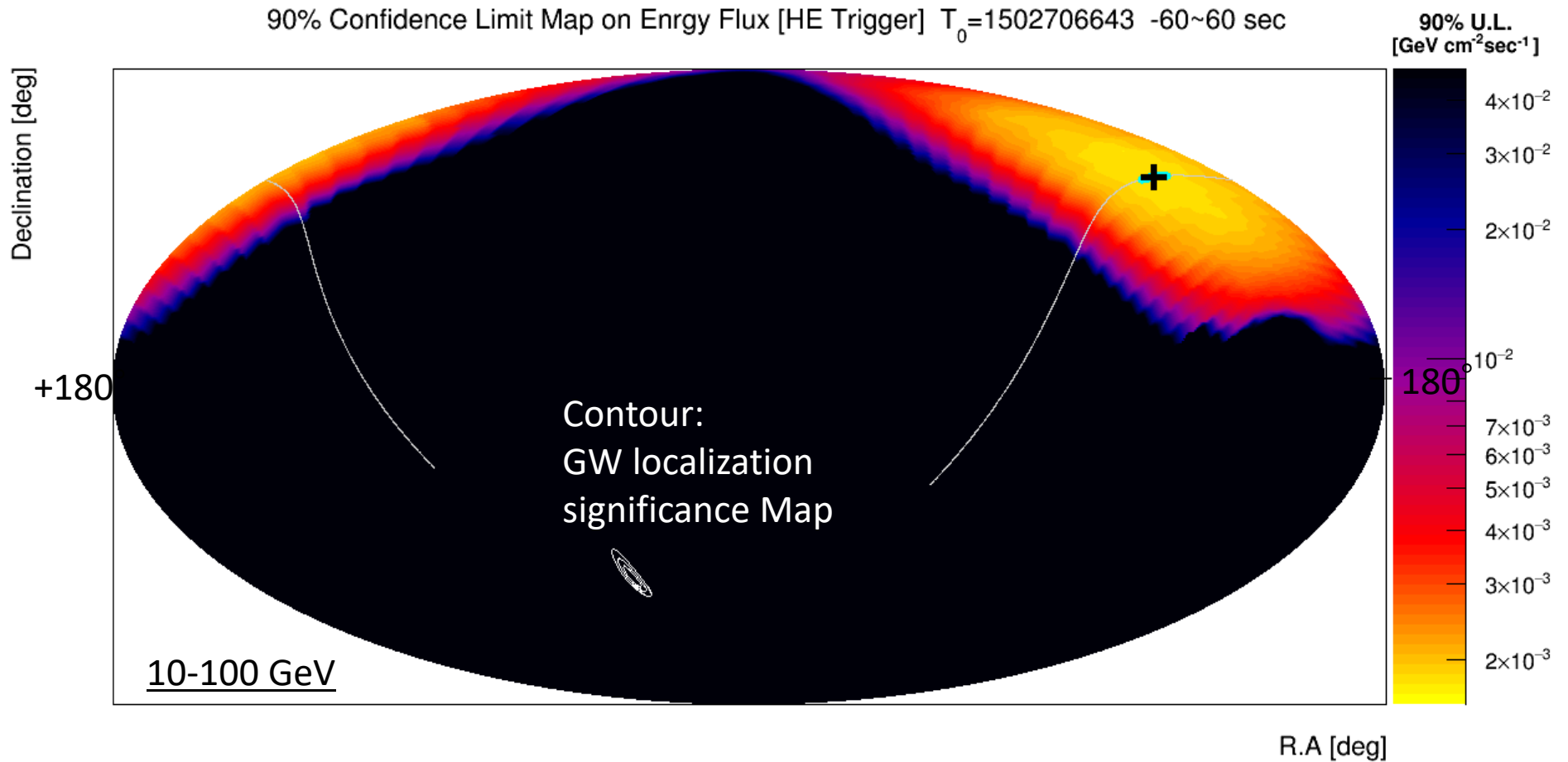
Preliminary  
O. Adriani et al., in prep.



CALET observation was out of localized region of LIGO event.

# 90% CL Upper limit for GW170814 counterpart search

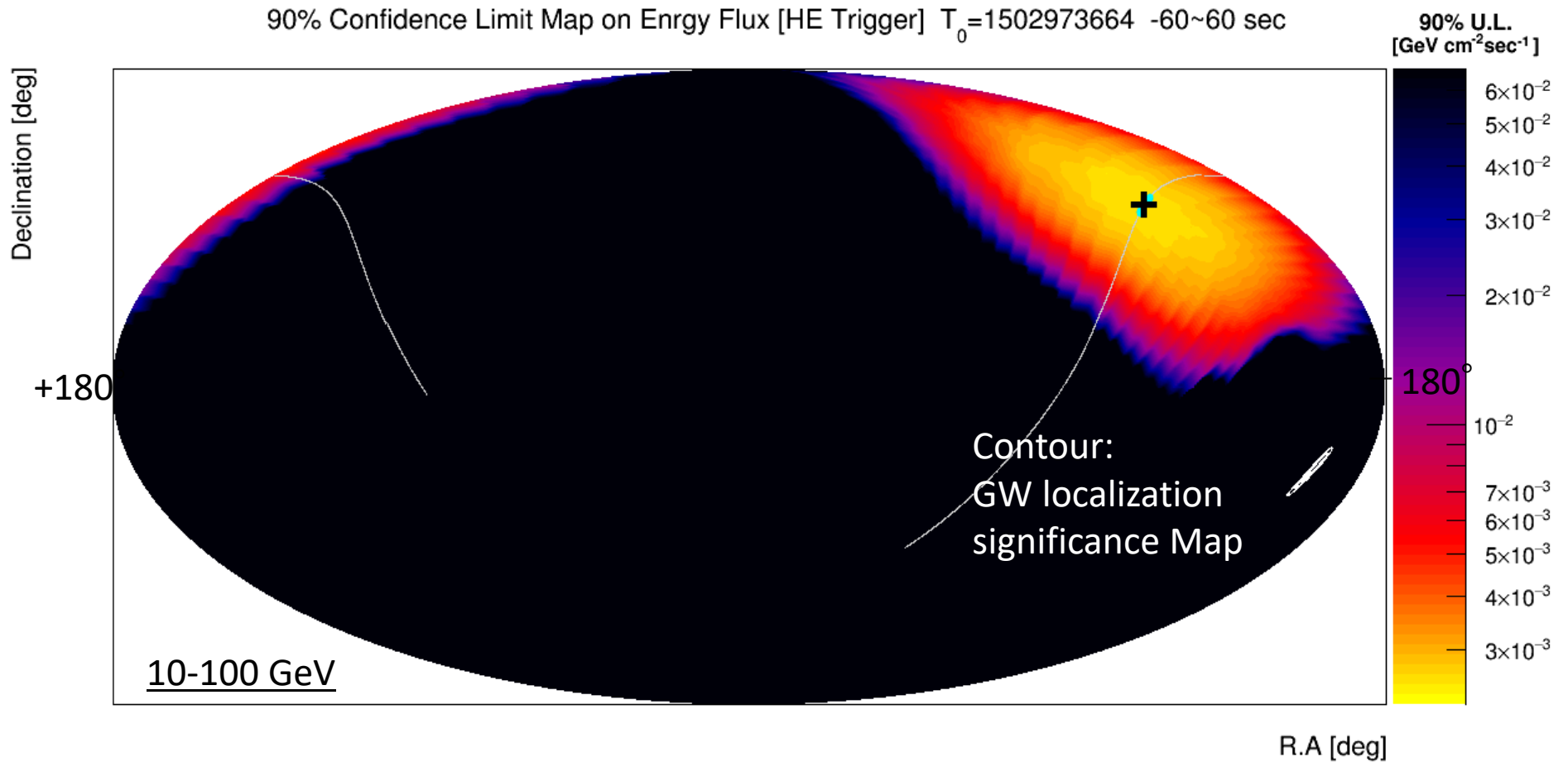
Preliminary  
O. Adriani et al., in prep.



CALET observation was out of localized region of LIGO event.

# 90% CL Upper limit for GW170817 counterpart search

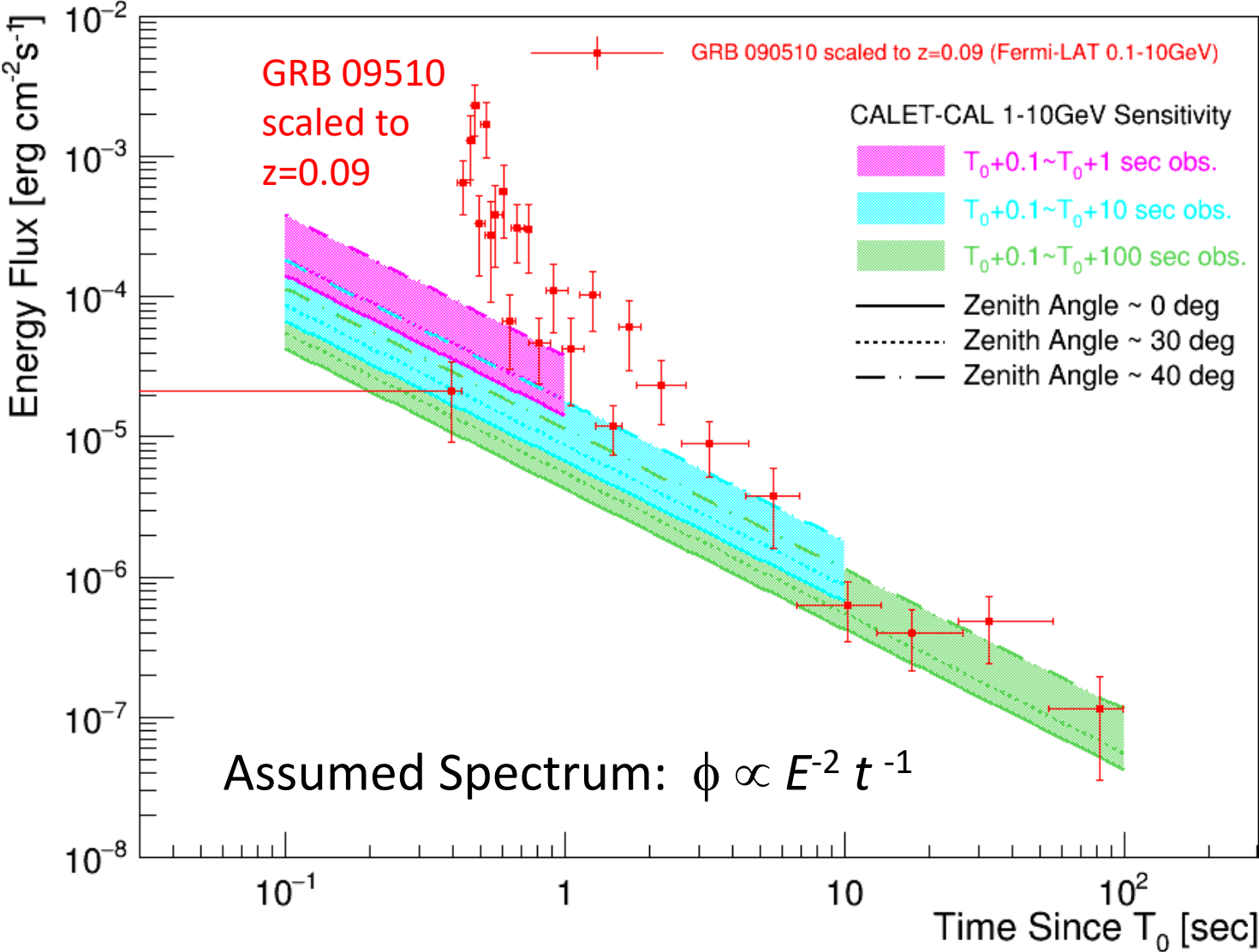
Preliminary  
O. Adriani et al., in prep.



CALET observation was out of localized region of LIGO event.

# CALET Sensitivity to GeV Gamma-Rays

Short GRBs accompanied by GeV gamma-ray emissions could be detected by CALET-CAL given the closeness of GW candidates.



Preliminary:  
O. Adriani et al., in prep.

# Summary & Prospects

Preliminary  
O. Adriani et al., in prep.

1. CALET was successfully launched on Aug. 19, 2015, and the detector is being very stable for observation since Oct. 13, 2015.
2. As a result of GW151226 counterpart search in GeV gamma-rays, CALET-CAL observation constrains 15% of LIGO localization map by 90% upper limit flux of  $9.3 \times 10^{-8} \text{ erg cm}^{-2} \text{ sec}^{-1}$  (1-10GeV).
3. GeV gamma-ray counterpart of other GW events during O1&O2 have been performed and limits are set if there are overlap between our FOV and LIGO/Virgo localization map.
4. Its sensitivity was validated with diffuse and point-source observations.
5. Due to closeness of GW candidates, FOV coverage is more important than deepness of counterpart search assuming on-axis short GRBs as candidates.
6. Automated pipeline to search for gamma-ray transient was also developed and is being implemented.  
**⇒ Transient objects such as GW counterparts and GRBs, as well as flaring point sources will be monitored.**

*This work is partially supported by JSPS Grant-in-Aid for Scientific Research (S) Number 26220708, JSPS Grant-in-Aid for Scientific Research (B) Number 17H02901, JSPS Grant-in-Aid for Scientific Research (C) Number 16K05382.*



National Aeronautics and Space Administration  
Goddard Space Flight Center

Fermi • HEASARC • Sciences and Exploration



# Celebrating 10 Years of Fermi

June 11, 2018

Home    What is Fermi    Science    Fermi@10    Support Center    Mission Page    Students/Teachers

## Latest News

**Mar 20, 2018**

### Fermi Spacecraft Operational Anomaly

At 5:11 UT on March 16, Fermi encountered an issue with the solar array drive that caused the observatory to go into safe hold. In this mode, the instruments are powered off, and thus science data taking has stopped. Initial investigation suggests that one of the solar panels is stuck.

Investigation into the cause of the anomaly is ongoing and will continue for some time. We are exploring options to resume some science operations with a fixed solar panel which would run while the anomaly investigations are ongoing. The team is planning to start a return to science ops next week, to run in parallel with the ongoing engineering investigation.

### GeV sky

- Agile
- CALET/CAL
- DAMPE (Wukong)